Nat. Hazards Earth Syst. Sci. Discuss., 3, 5191–5208, 2015
www.nat-hazards-earth-syst-sci-discuss.net/3/5191/2015/
doi:10.5194/nhessd-3-5191-2015

Natural Hazards and Earth System Sciences
Open Access
Discussions

Probabilistic tsunami hazard assessment for the Makran region with focus on maximum magnitude assumption

A. Hoechner, A. Y. Babeyko, and N. Zamora

GFZ German Research Centre for Geosciences, Potsdam, Germany

Received: 11 June 2015 – Accepted: 6 August 2015 – Published: 1 September 2015

Correspondence to: A. Hoechner (hoechner@gfz-potsdam.de)

Published by Copernicus Publications on behalf of the European Geosciences Union.

Abstract

Despite having been rather seismically quiescent for the last decades, the Makran subduction zone is capable of hosting destructive earthquakes and tsunami. In particular, the well-known thrust event in 1945 (Balochistan earthquake) led to about 4000 casualties. Nowadays, the coastal regions are more densely populated and vulnerable to similar events. Furthermore, some recent publications discuss rare but significantly larger events at the Makran subduction zone as possible scenarios. We analyze the instrumental and historical seismicity at the subduction plate interface and generate various synthetic earthquake catalogs spanning 300 000 years with varying magnitude–frequency relations. For every event in the catalogs we compute estimated tsunami heights and present the resulting tsunami hazard along the coasts of Pakistan, Iran and Oman in the form of probabilistic tsunami hazard curves. We show how the hazard results depend on variation of the Gutenberg–Richter parameters and especially maximum magnitude assumption.

1 Introduction

A subduction zone along the Makran coast was proposed for the first time by Stoneley fourty years ago (Stoneley, 1974) and found to be in agreement with seismicity (Quittmeyer and Jacob, 1979) as well field observations (Page et al., 1979). There is no clear trench developed where the Arabian plate subducts beneath the Eurasian plate, and rather low seismicity characterizes the interplate seismogenic zone. It hosted as largest recorded earthquake an event with $M_w = 8.1$ in 1945 (Byrne et al., 1992). For these reasons, and due to its low population density, it is not as prominent in scientific literature as other tsunami-prone subduction zones. Nevertheless, the Makran or Balochistan event mentioned above caused the tsunami with the highest number of fatalities of 4000 in the Indian Ocean region prior to the 2004 Sumatra–Andaman earthquake (Heidarzadeh et al., 2008b).

NHESSD
3, 5191–5208, 2015

Some publications assessed the tsunami hazard for the coast of Iran, Pakistan and Oman originating from the subduction process: Heidarzadeh et al. (2008a, c) performed deterministic analyses based on 5 magnitude 8.1 events and 6 magnitude 8.3 events respectively, and Heidarzadeh and Kijko (2010) carried out a probabilistic study based on 3 magnitude 8.1 sources associated with probabilities to propose what they labeled a "first generation" probabilistic tsunami hazard assessment (PTHA) for the region.

The two largest earthquakes of the past 50 years, the 2004 Sumatra–Andaman earthquake, and the 2011 Tohoku earthquake both were against expectations of most of the scientific community: since such huge events had not been observed before at these locations, they had not been accounted for. Since then, increased attention has been given to the question of what maximum magnitude can be expected for the different subduction zones. For instance, Schellart and Rawlinson (2013) tried to find correlations between 24 parameters related to subduction (geometry, geology, kinematics, dynamics) and maximum magnitude on a global scale, and found that some parameters appear to lie in a limited band for subduction segments capable of very large events. They concluded that Makran falls into the set of regions with events larger than $M_w = 8.5$ possible. McCaffrey (2008) states that present evidence cannot rule out that any subduction zone may produce a magnitude 9 event, based on statistical analysis of Monte-Carlo simulations. Smith et al. (2013) performed a thermo-mechanical analysis to assess the seismogenic potential of the Makran subduction zone. They found that the thick sediment cover leading to high plate boundary temperatures at the deformation front makes the megathrust potentially seismogenic to a shallow depth, and the low dip angle leads to a wide seismogenic zone, resulting in an upper estimate for a seaward earthquake of $M_w = 8.7–9.2$.

In this study, we perform a PTHA using synthetic earthquake catalogs based on an analysis of the seismicity in order to capture the hazard from the full spectrum of possible earthquakes for the coast lines of Iran, Pakistan and Oman. Since recent studies suggest that maximum magnitude for Makran might be significantly higher than

NHESSD
3, 5191–5208, 2015

previously thought, special focus is on the consequences of the assumptions made for maximum magnitude.

2 Methods

Our approach is similar to the one described by Sørensen et al. (2012): first we determine the seismicity in the area of interest, then we generate synthetic earthquake catalogs spanning a much larger time than instrumental and even historic record in order to get stable statistics. For every single event we run a tsunami model to get estimated maximum wave heights along the coast line. These are used to compute tsunami hazard and finally to generate various hazard plots. The difference to the approach mentioned above is, that instead of defining randomly distributed single-fault events of a certain parameter range within the source areas, we project the synthetic earthquake catalog hypocenters to the subduction plate interface and employ a realistic slip distribution. The procedure is described in more detail in the following sections.

2.1 Seismicity

From the various published catalogs for the Middle East we select the most recent one by Zare et al. (2014), which has been compiled in the framework of the Global Earthquake Model (GEM) and includes all historical, early and modern instrumental events up to 2006 with unified moment magnitude. For the Makran region, the authors suggest a magnitude of completeness of $M_c = 5.5$ after 1920 and $M_c = 4.5$ after 1963. We select only those events lying in the area covered by the plate interface described below.

The seismicity is determined using the procedure by Kijko and Smit (2012) using their Matlab code "aue.m" and applying magnitudes of completeness following Zare et al. (2014) using the events from 1919–1963 and 1964–2006 with an assumed magnitude error of 0.2. The resulting b value is 0.82. The code "aue.m" also generates cu-

NHESSD
3, 5191–5208, 2015

mulative seismicity rates (lambda) based on Gutenberg–Richter–Bayes (GRB) statistics which include uncertainty for the magnitude–frequency relations. We use this distribution for the generation of the reference synthetic catalog (RSC).

The plate interface geometry, which is neither available via the RUM model (Gudmundsson and Sambridge, 1998) nor Slab1.0 (Hayes et al., 2012) is obtained by rotating the profile by Smith et al. (2013) around 61.75°/38.0° Lon/Lat which keeps its upper tip close to the deformation front from the same publication. The resulting plate interface excludes the clearly non-subduction seismicity to the west and east (Fig. 1), the lower edge is at 70 km depth.

2.2 Synthetic catalog

The synthetic catalogs each span 300 000 years and are created by randomly generating events within the area spanned by the plate interface geometry with magnitudes according to the inferred magnitude–frequency relation (and exponential inter-event time distribution). All the events are assumed to be thrust events at the subduction interface. Of course, this assumption would be unacceptable for a seismic hazard analysis, since part of the seismicity is related to crustal and intraplate earthquakes in the slab. But in case of a tsunami hazard assessment it is not such an issue: all the events on land do not cause any tsunami at all, whereas most of the large, tsunamigenic events in the sea can reasonably be assumed to be thrust interplate events (strike-slip events have lower impact). The reason why we do include the area on land is to get a better picture of the seismicity (which is low and furthermore not well recorded) for the determination of the magnitude–frequency relation. The maximum magnitude for the RSC is set to 9.0. It is important to stress that this value is not the most likely one, but it has to be considered as end-member assumption.

In addition to the RSC, other catalogs are generated by varying the Gutenberg–Richter a and b values, a combination thereof resulting in a rotation about the rate at $M = 6$, and, most importantly, the maximum magnitude (Fig. 2).

NHESSD
3, 5191–5208, 2015

The hypocenters of the catalog events are projected to the subduction interface, which consists of subfaults of about 20 km edge length. These are activated based on scaling relations for length and width in dependence of magnitude by Blaser et al. (2010) (reverse orthogonal) with a slip distribution according to Geist and Dmowska (1999) along dip and linear tapering of 20 % towards the lateral edges.

2.3 Tsunami model

For every subfault, the sea floor deformation resulting from 1 m dip-slip (rake angle is set to 90°) is calculated for the homogeneous elastic half-space and used as input for the tsunami code easyWave (Babeyko, 2012), which propagates the initial condition to compute wave height time series for points along the coast in about 50 m water depth (tsunami Green's functions). Up to this water depth it is possible to assume linear conditions for our purpose (Miranda et al., 2014), so that the unit time series can be combined according to the slip distribution. This enables us to compute a large number of scenarios with little computational effort. The maximum of the time series is extrapolated to the shore using Green's law (Kamigaichi, 2009) to obtain peak coastal tsunami amplitude (PCTA) at points of interest (POI). Bathymetry is from GEBCO (2008) with 30 arcsec resolution.

2.4 Tsunami hazard

For each point of interest, the number of exceedances of a certain wave height in a catalog is counted and divided by catalog time span to obtain annual probabilities. Probabilities for larger time spans and percentiles are calculated using Poisson statistics. Analogous for probability of exceedance (POE) anywhere in a region (counting exceedances anywhere within a subset of POI). The probabilistic tsunami height (PTH) is defined as the wave height which is expected once in a certain time (return period) (Bernard and Robinson, 2009; Sørensen et al., 2012).

NHESSD
3, 5191–5208, 2015

3 Results

Figure 3 shows some tsunami hazard measures for Iran and Pakistan for the RSC. According to the left panel, PTH for some specific location in the central region is around 12 m in 5000 years and 2 m in 500 years, but the PTH for the whole coast line as one is much higher, about 21 and 9 m respectively (circles with bars). The central panel shows PTH as a function of time for the whole coastline and for some cities along the coast. Jiwani (at 61.7° Lon) has the highest hazard, since it is exposed to more events than the cities of Jask or Ormara at the boundaries of the subduction zone. The circles correspond to the circles in the left panel. The right panel shows the POE at one or more locations as function of PCTA. The squares denote POE for 2 m/50 y, 8 m/500 y and 15 m/5000 y and are used for comparison in the summarizing Figs. 5 and 6. The dashed lines are the 15th and 85th percentiles and reflect fluctuations due to stochastical catalog generation.

Figure 4 shows the same plots for the exposed coast line of Oman. The hazard for Muscat (23.6° Lat) and Sur (22.6° Lat) is comparable to the one for Chabahar in Iran, but the cumulative hazard for Oman is lower, since only the events in the western part have a heavy impact on Oman.

The effect of assumed maximum magnitude for the synthetic seismic catalog on tsunami hazard is shown in Fig. 5, for Iran and Pakistan on the left side and for Oman on the right side, as PTH in the upper and as POE in the lower panels. The low-level short-term hazard is dominated by the large number of smaller events, while the high-level long-term hazard very strongly depends on the maximum magnitude. For instance, for Iran and Pakistan, the probability of exceeding 15 m in 5000 years increases from 21 % for M_{max} = 8.2 to 75 % for M_{max} = 8.6 and 93 % for M_{max} = 9.0.

Similarly, Fig. 6 shows the dependence of tsunami hazard on magnitude–frequency relations (for Iran and Pakistan and Oman together). Throughout Figs. 3 to 6, circles and squares are corresponding. Numerical values are listed in the Supplement.

NHESSD
3, 5191–5208, 2015

4 Discussion

Due to the rather low seismic activity, the tsunami hazard for Makran is generally lower than for other, seismically more active subduction zones, especially concerning short-term hazard. However, on the long-term, events with potentially catastrophic impact lead to significant hazard, meaning that risk mitigation efforts and early warning measures should be further developed and implemented.

Our estimations of tsunami hazard should not be considered as final. We discuss some of the factors affecting our results. The randomness of the synthetic seismic catalog: this is estimated by computing the 15th and 85th percentiles and is rather low due to the length of the catalogs of 300 000 years. Assumptions for scaling relations and slip distribution: these could have high impact on single events, where more complicated things like asperities can arise. Averaged over the whole catalog, the effect should be moderate. Projection of all events to the plate interface: although inadequate for seismic hazard assessment, for tsunami hazard assessment this assumption leads to a more conservative view as discussed in Sect. 2.2. Splay-faulting: not considered, could increase hazard. Tsunami modeling: we did not compute inundation maps and run-up which would be useful for specific scenarios, instead we estimated coastal wave heights as described in Sect. 3, which are adequate for hazard assessment and early warning purposes. Hazard could be increased by (submarine) landslides, possibly triggered by earthquakes. This could be handled in modeling, but due to even rarer occurrence than for earthquakes it is difficult to assign probabilities. In our opinion, the largest influence stems from uncertainty of the maximum magnitude, which we tried to assess in this study.

We now compare our results to findings by Heidarzadeh and Kijko (2010). For Jiwani, they report probabilities of exceeding 1, 3 and 5 m over a 50 year period of about 42, 18 and 18 %. Their "first generation" study contains only 3 scenarios with identical magnitude of $M_w = 8.1$ (all affecting Jiwani). This rough discretization leads to the same value for 3 and 5 m exceedance probabilities and also implies that these values

NHESSD
3, 5191–5208, 2015

should not be compared to our result for the specific location, but to our probability of exceedance anywhere within some coastal region. For a maximum magnitude of $M_{max} = 8.2$ our results are 46, 24 and 14 %, for the coast line of Iran and Pakistan, which is in good agreement with the result above. For $M_{max} = 8.6$ the values increase rather moderately to 48, 28 and 19 %. As mentioned in Sect. 3, this short-term hazard is dominated by smaller events, so that higher M_{max} has limited effect, but the long-term hazard is heavily affected by M_{max}.

An interesting question concerns the possible segmentation of the Makran subduction zone. The seismicity varies strongly across the Makran region. While large thrust events are known to have occurred in the eastern part, there is no proof of historic events in western Makran (Musson, 2009). Byrne et al. (1992) discussed whether this should be interpreted as aseismic sliding in the west, or rather complete locking of the interface (with opposite hazard consequences). They concluded that the occurrence of uplifted Holocene marine terraces along the coast as well as the continuity of the deformation front indicate that the latter is more probable. However, even assuming locking, it is still not clear whether a giant event rupturing the whole plate interface at once is possible or whether the segmentation would favor sub-events involving only part of the interface. In this study we did not consider segmentation of the subduction zone, further studies with refined seismicity models taking segmentation into account are desirable.

Several things can be done to increase resilience against tsunami: education of the population, planning of evacuation procedures, protection of high-risk facilities and installation of efficient early-warning systems. The traditional approach for tsunami early warning is based on seismic methods, but especially for Iran and Pakistan, a GNSS (Global Navigation Satellite System) based approach should be considered (Sobolev et al., 2007; Hoechner et al., 2008; Babeyko et al., 2010; Hoechner et al., 2013).

The Supplement related to this article is available online at doi:10.5194/nhessd-3-5191-2015-supplement.

NHESSD
3, 5191–5208, 2015

Acknowledgements. Funding was by CEDIM for A. Hoechner and by GeoSim and Helmholtz Association for N. Zamora.

The article processing charges for this open-access publication were covered by a Research Centre of the Helmholtz Association.

References

Babeyko, A. Y.: easyWave, available at: http://trac.gfz-potsdam.de/easywave (last access: 17 February 2015), 2012.

Babeyko, A. Y., Hoechner, A., and Sobolev, S. V.: Source modeling and inversion with near real-time GPS: a GITEWS perspective for Indonesia, Nat. Hazards Earth Syst. Sci., 10, 1617–1627, doi:10.5194/nhess-10-1617-2010, 2010.

Bernard, E. N. and Robinson, A. R.: Tsunamis, Harvard University Press, London, UK, 450 pp., 2009.

Blaser, L., Krüger, F., Ohrnberger, M., and Scherbaum, F.: Scaling relations of earthquake source parameter estimates with special focus on subduction environment, B. Seismol. Soc. Am., 100, 2914–2926, doi:10.1785/0120100111, 2010.

Byrne, D. E., Sykes, L. R., and Davis, D. M.: Great thrust earthquakes and aseismic slip along the plate boundary of the Makran Subduction Zone, J. Geophys. Res.-Sol. Ea., 97, 449–478, doi:10.1029/91JB02165, 1992.

GEBCO: General Bathymetric Chart of the Oceans (GEBCO), available at: http://www.gebco.net/ (last access: 17 February 2015), 2008.

Geist, E. L. and Dmowska, R.: Local tsunamis and distributed slip at the source, Pure Appl. Geophys., 154, 485–512, doi:10.1007/s000240050241, 1999.

GEM: Global Earthquake Model, available at: http://www.globalquakemodel.org/ last access: 9 June 2015.

Gudmundsson, Ó. and Sambridge, M.: A regionalized upper mantle (RUM) seismic model, J. Geophys. Res., 103, 7121–7136, doi:10.1029/97JB02488, 1998.

Hayes, G. P., Wald, D. J., and Johnson, R. L.: Slab1.0: a three-dimensional model of global subduction zone geometries, J. Geophys. Res.-Sol. Ea., 117, B01302, doi:10.1029/2011JB008524, 2012.

NHESSD

3, 5191–5208, 2015

Heidarzadeh, M. and Kijko, A.: A probabilistic tsunami hazard assessment for the Makran subduction zone at the northwestern Indian Ocean, Nat. Hazards, 56, 577–593, doi:10.1007/s11069-010-9574-x, 2010.

Heidarzadeh, M., Pirooz, M. D., Zaker, N. H., and Synolakis, C. E.: Evaluating tsunami hazard in the northwestern Indian Ocean, Pure Appl. Geophys., 165, 2045–2058, doi:10.1007/s00024-008-0415-8, 2008a.

Heidarzadeh, M., Pirooz, M. D., Zaker, N. H., Yalciner, A. C., Mokhtari, M., and Esmaeily, A.: Historical tsunami in the Makran Subduction Zone off the southern coasts of Iran and Pakistan and results of numerical modeling, Ocean Eng., 35, 774–786, doi:10.1016/j.oceaneng.2008.01.017, 2008b.

Heidarzadeh, M., Pirooz, M. D., Zaker, N. H., and Yalciner, A. C.: Preliminary estimation of the tsunami hazards associated with the Makran subduction zone at the northwestern Indian Ocean, Nat. Hazards, 48, 229–243, doi:10.1007/s11069-008-9259-x, 2008c.

Hoechner, A., Babeyko, A. Y., and Sobolev, S. V.: Enhanced GPS inversion technique applied to the 2004 Sumatra earthquake and tsunami, Geophys. Res. Lett., 35, L08310, doi:10.1029/2007GL033133, 2008.

Hoechner, A., Ge, M., Babeyko, A. Y., and Sobolev, S. V.: Instant tsunami early warning based on real-time GPS – Tohoku 2011 case study, Nat. Hazards Earth Syst. Sci., 13, 1285–1292, doi:10.5194/nhess-13-1285-2013, 2013.

Kamigaichi, O.: Tsunami forecasting and warning, in: Encyclopedia of Complexity and Systems Science, edited by: Meyers, R. A., Springer, New York, 9592–9618, 2009.

Kijko, A. and Smit, A.: Extension of the Aki-Utsu b-value estimator for incomplete catalogs, B. Seismol. Soc. Am., 102, 1283–1287, doi:10.1785/0120110226, 2012.

McCaffrey, R.: Global frequency of magnitude 9 earthquakes, Geology, 36, 263–266, doi:10.1130/G24402A.1, 2008.

Miranda, J. M., Baptista, M. A., and Omira, R.: On the use of Green's summation for tsunami waveform estimation: a case study, Geophys. J. Int., 199, 459–464, doi:10.1093/gji/ggu266, 2014.

Musson, R. M. W.: Subduction in the Western Makran: the historian's contribution, J. Geol. Soc., 166, 387–391, doi:10.1144/0016-76492008-119, 2009.

Page, W. D., Alt, J. N., Cluff, L. S., and Plafker, G.: Evidence for the recurrence of large-magnitude earthquakes along the Makran coast of Iran and Pakistan, Tectonophysics, 52, 533–547, 1979.

NHESSD
3, 5191–5208, 2015

Quittmeyer, R. C. and Jacob, K. H.: Historical and modern seismicity of Pakistan, Afghanistan, northwestern India, and southeastern Iran, B. Seismol. Soc. Am., 69, 773–823, 1979.
Schellart, W. P. and Rawlinson, N.: Global correlations between maximum magnitudes of subduction zone interface thrust earthquakes and physical parameters of subduction zones, Phys. Earth Planet. In., 225, 41–67, doi:10.1016/j.pepi.2013.10.001, 2013.
Smith, G. L., McNeill, L. C., Wang, K., He, J., and Henstock, T. J.: Thermal structure and megathrust seismogenic potential of the Makran subduction zone, Geophys. Res. Lett., 40, 1528–1533, doi:10.1002/grl.50374, 2013.
Sobolev, S. V., Babeyko, A. Y., Wang, R., Hoechner, A., Galas, R., Rothacher, M., Sein, D. J., Schröter, J., Lauterjung, J., and Subarya, C.: Tsunami early warning using GPS-shield arrays, J. Geophys. Res., 112, B08415, doi:10.1029/2006JB004640, 2007.
Sørensen, M. B., Spada, M., Babeyko, A., Wiemer, S., and Grünthal, G.: Probabilistic tsunami hazard in the Mediterranean Sea, J. Geophys. Res.-Sol. Ea., 117, B01305, doi:10.1029/2010JB008169, 2012.
Stoneley, R.: Evolution of the continental margins bounding a former southern Tethys, in: The Geology of the Continental Margins, 1st edn., edited by: Burk, C. A. and Drake, C. L., Springer-Verlag, Berlin Heidelberg, available at: http://www.springer.com/us/book/9783662011430#aboutBook (last access: 11 February 2015), 1974.
Zare, M., Amini, H., Yazdi, P., Sesetyan, K., Demircioglu, M. B., Kalafat, D., Erdik, M., Giardini, D., Asif Khan, M., and Tsereteli, N.: Recent developments of the Middle East catalog, J. Seismol., 18, 749–772, doi:10.1007/s10950-014-9444-1, 2014.

NHESSD
3, 5191–5208, 2015

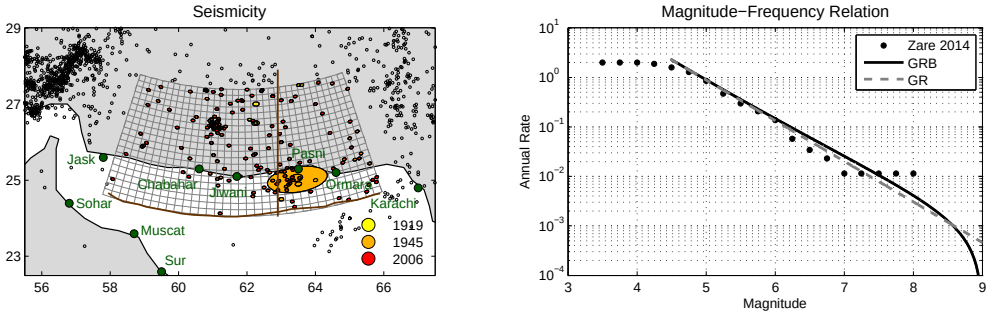

Figure 1. Left: seismicity (Zare et al., 2014), color of the events corresponds to year and size is by scaling relations (Blaser et al., 2010). The brown lines are the profile and deformation front by Smith et al. (2013), grey is the used subduction interface. Right: inferred magnitude–frequency relation. Solid: Gutenberg–Richter–Bayes (used), grey: Gutenberg–Richter (for comparison).

NHESSD
3, 5191–5208, 2015

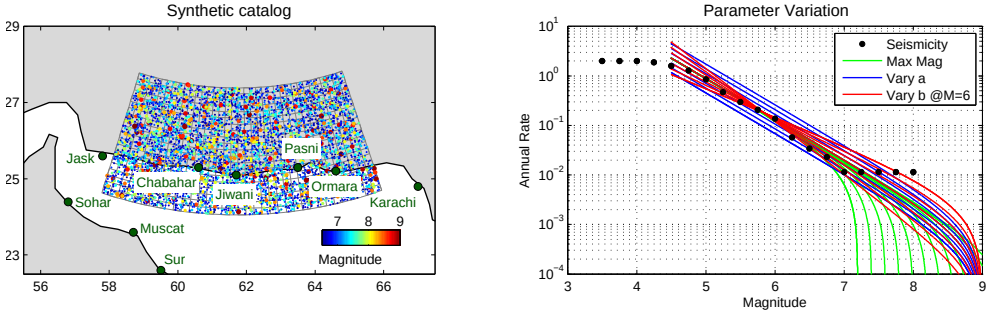

Figure 2. Left: first 5000 events in the reference synthetic catalog color coded by magnitude. The whole catalog spanning 300 000 years contains about 20 000 events. Right: parameter range tested for the magnitude–frequency relation.

NHESSD
3, 5191–5208, 2015

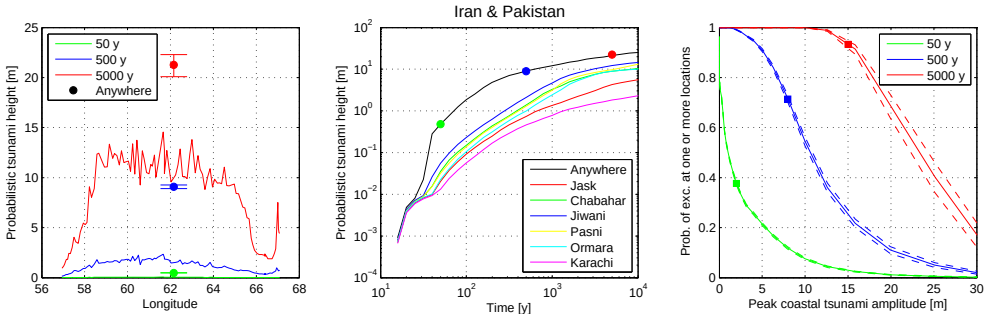

Figure 3. Left: probabilistic Tsunami Height (PTH) for Iran and Pakistan along Longitude (colored lines) and for the whole coast at once (circles with 15th and 85th percentile bars). Center: PTH as function of time for selected cities (color) and the coastline as whole (black). Right: probability Of Exceedance (POE) as function of Peak Coastal Tsunami Amplitude (PCTA) for different time periods. Dashed: 15th/85th percentiles.

NHESSD
3, 5191–5208, 2015

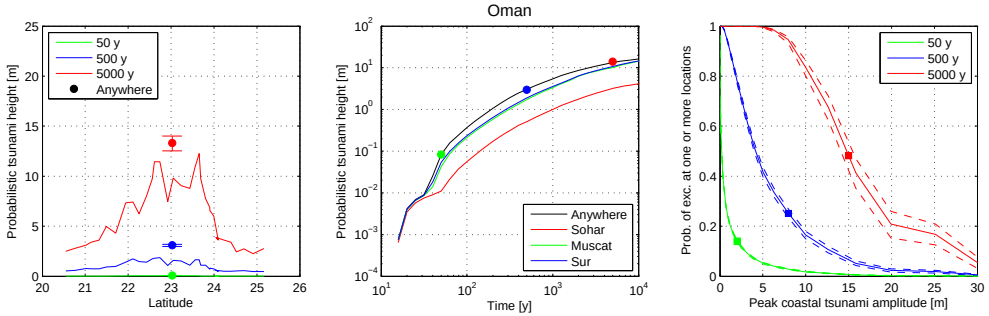

Figure 4. Same as Fig. 3 but for the exposed coast line of Oman.

NHESSD
3, 5191–5208, 2015

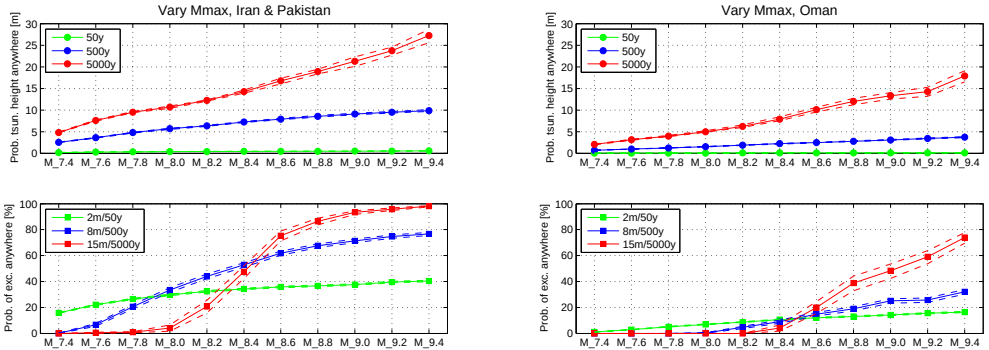

Figure 5. Influence of maximum magnitude assumption on tsunami hazard. Left: Iran and Pakistan. Right: Oman. Upper: probabilistic Tsunami Height (PTH). Lower: probability Of Exceedance (POE).

NHESSD
3, 5191–5208, 2015

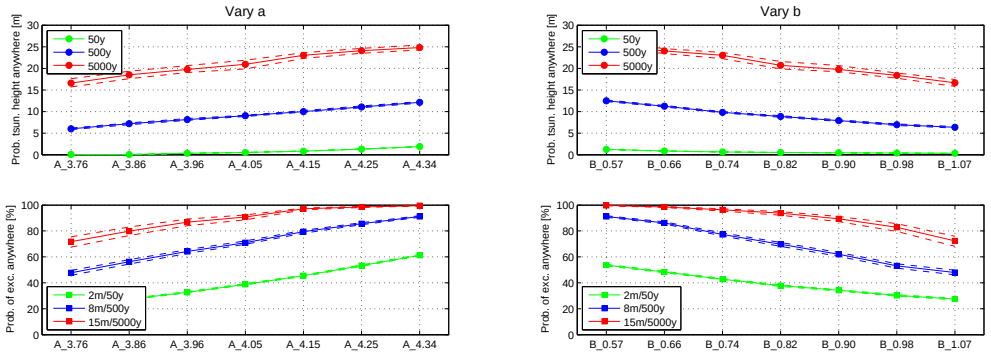

Figure 6. Influence on PTH (upper panels) and POE (lower panels) from varying a-parameter (seismic rate) (left) and b-parameter (right) around $M = 6$.

NHESSD
3, 5191–5208, 2015